Available online at www.sciencedirect.com

SCIENCE DIRECT

International Journal of Thermal Sciences 44 (2005) 235–244

International Journal of Thermal Sciences

www.elsevier.com/locate/ijts

A sequential algorithm of inverse heat conduction problems using singular value decomposition

José María Gutiérrez Cabeza [a], Juan Andrés Martín García [b], Alfonso Corz Rodríguez [c,*]

[a] *Department of Applied Physics of University of Cádiz, Escuela Politécnica Superior de Algeciras, Avda. Ramón Puyol, s/n, 11202 Algeciras (Cádiz), Spain*

[b] *Department of Electrical Engineering of University of Cádiz, Escuela Politécnica Superior de Algeciras, Avda. Ramón Puyol, s/n, 11202 Algeciras (Cádiz), Spain*

[c] *Department of Industrial and Civil Engineering of University of Cádiz, Escuela Politécnica Superior de Algeciras, Avda. Ramón Puyol, s/n, 11202 Algeciras (Cádiz), Spain*

Received 25 August 2003; received in revised form 2 February 2004; accepted 4 June 2004

Available online 5 November 2004

Abstract

This paper examines numerically and theoretically the application of truncated Singular Value Decomposition (SVD) in a sequential form. The Sequential SVD algorithm presents two tunable hyperparameters: the number of future temperature (r) and the rank of the truncated sensitivity matrix (p). The regularization effect of both hyperparameters is consistent with the data filtering interpretation by truncated SVD (reported by Shenefelt [Internat. J. Heat Mass Transfer 45 (2002) 67]). This study reveals that the most suitable reduced rank is "one". Under this assumption $(p = 1)$, the sequential procedure proposed, presents several advantages with respect to the standard whole-domain procedure: The search of the optimum rank value is not required. The simplification of the model is the maximum that can be achieved. The unique tunable hyperparameter is the number of future temperatures, and a very simple algorithm is obtained. This algorithm has been compared to: Function Specification Method (FSM) proposed by Beck and the standard whole-domain SVD. In this comparative study, the parameters considered have been: the shape of the input, the noise level of measurement and the size of time step. In all cases, the FSM and sequential SVD algorithm give very similar results. In one case, the results obtained by the sequential SVD algorithm are clearly superior to the ones obtained by the whole-domain algorithm.

Keywords: Inverse heat conduction; Singular value decomposition; Function specification method

1. Introduction

The Inverse Heat Conduction Problems (IHCP) are typical examples of "ill-posed problems". Several functions and parameters can be estimated in the IHCP: static and moving heating sources, properties, initial conditions, boundary conditions, optimal shape etc. This study is confined to the estimation of an unknown boundary condition. The unknown function can be stated as a surface flux, a surface temperature or a heat transfer coefficient. The lack of information is normally due to the difficulty to installing sensors in the boundary. This circumstance appears in applications where the boundary is inaccessible [1,2], in simulation of space vehicle re-entry [3], in metallurgic applications [4,5], etc. In order to recover the unknown time history, is necessary to obtain the additional information provided by remote temperature sensors placed at interior locations. As a consequence of the diffusive nature of heat flow, the thermal response at some distance of the boundary is damped and lagged with respect to the active input at the boundary. This implies that in many cases the problem presents a low or insufficient sensitivity. On the other hand, the relationship between the thermal response and the unknown input can be

* Corresponding author. Tel.: +34 952 137045, fax.: +34 952 137045
E-mail addresses: josemaria.gutierrez@uca.es (J.M. Gutiérrez Cabeza), juanandres.martin@uca.es (J.A. Martín García), alfonso.corz@uca.es (A. Corz Rodríguez).

1290-0729/$ – see front matter
doi:10.1016/j.ijthermalsci.2004.06.009

Nomenclature

$\boldsymbol{b}$	data vector
C	constant
c	coefficient, Eq. (10)
D	estimate of bias
$\mathbf{H}$	partition of sensitivity matrix, Eq. (12)
M	total number of time step
N	total number of estimated values
q	dimensionless heat flux
$\mathbf{q}$	heat flux vector
T	dimensionless temperature
$\mathbf{T}$	vector of calculated temperatures
T_0	initial condition
p	reduced rank
r	number of future time steps
t	dimensionless time
u	Gaussian random numbers (normalized)
$\mathbf{U}$	orthogonal matrix
$\mathbf{u}$	left singular vector
$\mathbf{V}$	orthogonal matrix
$\mathbf{v}$	right singular vector
$\mathbf{S}$	diagonal matrix
S	estimate of total error
x	dimensionless coordinate
$\mathbf{X}$	sensitivity matrix
Y	measured temperature
$\mathbf{Y}$	vector of measured temperatures

Greek symbols

β	coefficient, Eq. (10)
Δt	time step size
ε	random error
ϕ	response to a unit step change
$\Delta\phi$	response to a unit pulse
λ	singular value
σ	standard deviation

Subscripts

i	at time t_i
fut	future components
past	previous components
red	reduced rank approximation

Superscripts

$\widehat{}$	estimated
T	transposed

expressed through a sensitivity matrix. The sensitivity matrix tends to be quasi-singular. This explains the principal difficulty of the IHCP: the estimation tends to be unstable due to the great amplification of measurements errors. This difficulty is increased when the time interval between measurements is reduced. This particular point can be discussed considering the exact solution of Burggraf [6].

Fortunately, many methods have been reported to solve IHCPs, among the more versatile methods (applicable to solve multidimensional and non-linear IHCP) the following can be mentioned: Tikhonov regularization [7], iterative regularization [8], mollification [9], and the function specification method (FSM) [6]. The first two methods are considered as "whole domain" because all the measured temperature data are used in order to estimate simultaneously all the components of the unknown input. In these methods, the sensitivity matrix can be of great dimensions. In contrast, the last two methods are sequential. Therefore, only a little part of available measurement is used in each step and only one component of the unknown input is estimated at each step. This fact can be an advantage in an on-line process. A considerable number of contributions have been published considering combinations, modifications and comparisons of the previous methods. Beck and Murio [10] presented a new method that combines the function specification method of Beck with the regularization technique of Tikhonov. Murio and Paloschi [11] propose a combined procedure based on a data filtering interpretation of the mollification method and FSM. Zabaras and Lyu [12] combine the Boundary Element Method (BEM) in conjunction with Beck's sensitivity analysis and least-squares method. Blanc et al. [13], introduced a modification in the FSM, so that the new algorithm uses a time-variable number of future temperatures. Beck et al. [14] compare the FSM, the Tikhonov regularization and the iterative regularization, using experimental data.

On the other hand, there are other procedures that have been used in other applications (economics, signal processing, image reconstruction, etc.), and have also been applied successfully in IHCP in order to get a stable estimation. In this frame, the well-known Kalman filtering technique [15] has been used to resolve linear and non-linear IHCP [16, 17]. The use of an artificial neural network (ANN) has also been considered in the IHCP [18]. Another effective technique to solve ill-posed problems is based in the Singular Value Decomposition (SVD) of an ill conditioned matrix [19]. Martin and Dulikravich [20,21] combine SVD in conjunction with the BEM to resolve inverse problems in steady heat conduction. The inverse problem in transient heat conduction has also been studied using SVD, for example, Shen [22] compares the results of the truncated SVD methods with the corresponding by Tikhonov's regularization. Muniz et al. [23], consider the estimation of an initial condition, and compare three methods: Tikhonov regularization, maximum entropy principle and truncated SVD. They found out that if the initial condition presents a spatial distribution with harmonic form, the truncated SVD presents the best approximate solution. However, in other tests the Max.-Entropy methods present the best reconstruction. More recently, Shenefelt [24] presented the data filtering interpretation by the truncated SVD in IHCP. In all these previous authors, the truncated SVD method was applied as a whole domain procedure.

This study examines numerically and theoretically the application of truncated SVD in a sequential form. The new matrix structure is presented. Although the estimations for $p > 1$ are good, it is found that the corresponding optimum r-value can be too large. Only when $p = 1$ the optimum r-value is similar (or equal) to the one required by the future sequential method. Under this assumption ($p = 1$), the simplification of the model (in each step) is the maximum that can be achieved. This fact permits the derivation of a very simple algorithm. This method is compared to the FSM of Beck and to the standard whole-domain SVD. In this comparison, the parameters considered have been: the shape of the input, the size of time step and the level of noise in the measurement.

In the following section we formulate the direct problem, which will be used in the inverse problem (Section 3) in order to generate synthetically the measured temperatures. The primary objective of this section is to present the sequential SVD algorithm (Section 3.3), nevertheless it requires a previous consideration of the whole domain SVD algorithm (Section 3.2). The well-known FSM of Beck is briefly outlined in Section 3.1. Section 4 discusses the regularization effects of the hyperparameters p and r. On the other hand, a total of five cases are analysed and compared by the three methods. Finally, the conclusions are exposed in Section 5.

2. Direct problem

We consider a transient, one-dimensional and linear heat conduction problem, represented in Fig. 1. The mathematical formulation is given by the differential equation (1a), the boundary conditions (1b), (1c) and the initial condition (1d).

$$\frac{\partial^2 T}{\partial x^2} = \frac{\partial T}{\partial t} \quad 0 \leqslant x \leqslant 1 \tag{1a}$$

$$-\frac{\partial T}{\partial x}\bigg|_{x=0} = q(t) \tag{1b}$$

$$-\frac{\partial T}{\partial x}\bigg|_{x=1} = 0 \tag{1c}$$

$$T(x,0) = T_0 = 0 \quad 0 \leqslant x \leqslant 1 \tag{1d}$$

The previous equations have been written in non-dimensional form. The boundary condition (1b) represents a dimensionless flux imposed at $x = 0$. This flux can be an arbitrary function. In the numerical simulation of this study, three different functions (test cases) will be considered. The response of the direct problem $T(x,t)$ can be calculated analytically [25] or numerically. We are interested in the response at $x = 1$, because it will be used in the next section in the inverse problem. In a linear problem, a linear dependence exist between the input (in this case $q(t)$) and the response

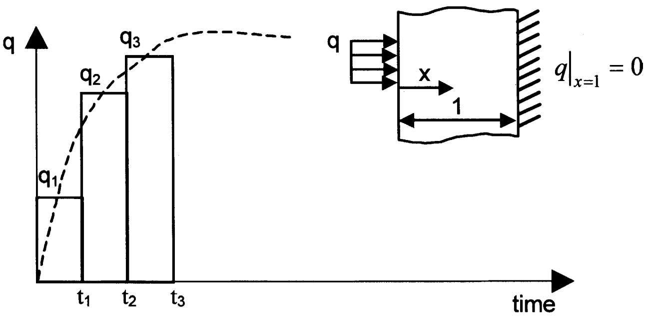

Fig. 1. Scheme of the 1D problem and boundary conditions.

(at $x = 1$). This dependence can be expressed analytically by the Duhamel integral [6]:

$$T(x,t) = \int_0^t q(s) \frac{\partial \phi(x, t-s)}{\partial t} + T_0 \tag{2}$$

where $\phi(x,t)$ represents the temperature response at location x for a unit step change (of flux) in the input, and T_0 is the initial condition (in this case it is 0). The analytical expression of $\phi(x,t)$ can be found in Ref. [6]. Considering that the objective in the inverse problem is the estimation of q in a discrete form, Eq. (2) can be approximated at time t_M as

$$T_M = T_0 + \sum_{n=1}^{M} q_n \Delta\phi_{M-n} \tag{3}$$

where subscripts denote the time instant considered. We note that the components q_i are assigned to time $t_{i+1/2}$, as it can be seen in Fig. 1. $\Delta\phi$ represents the temperature response to an unit pulse in the input, and hence: $\Delta\phi_i = \phi_{i+1} - \phi_i$. As it is evident $\Delta\phi_{i-j} = \partial T_i / \partial q_j$, consequently, it represents the sensitivity coefficient measured at time t_i with respect to component q_j. Obviously, the sensitivity coefficient will be zero when $i > j$. Considering the expression (3) for $M = 1, 2, \ldots,$ we obtain the following matrix equation

$$\mathbf{T} = [\mathbf{X}]\mathbf{q} + \mathbf{T}_0 \tag{4a}$$

where $\mathbf{T} = [T_1, T_2, \ldots, T_M]^{\mathrm{T}}$, $\mathbf{q} = [q_1, q_2, \ldots, q_M]^{\mathrm{T}}$, and the matrix $[\mathbf{X}]$ is

$$[\mathbf{X}] = \begin{bmatrix} \Delta\phi_0 & 0 & \ldots & 0 \\ \Delta\phi_1 & \Delta\phi_0 & \ldots & 0 \\ \vdots & \vdots & \ddots & \vdots \\ \Delta\phi_{M-1} & \Delta\phi_{M-2} & \ldots & \Delta\phi_0 \end{bmatrix} \tag{4b}$$

If the time history covers a long period of time, this matrix and the corresponding vector can be of a considerable dimension.

3. Inverse problem

In the inverse problem the available information is contained in the vector of measured temperatures from the interior of the body, in this case from $x = 1$. This vector will be noted as $\mathbf{Y}$. Because the measured temperatures Y_i are affected by errors, they are simulated using the discrete values of the analytical (or exact) temperature $T_i = T(1, t_i)$ (calculated in the direct problem) at times $t_i = i\Delta t$ (the time intervals of the measurements). Then, random errors ε_i are added according to: $Y_i = T_i + \varepsilon_i$, where $\varepsilon_i = Cu_i$. The random numbers u_i have been obtained using a random generator according to a normal (or Gaussian) distribution with zero mean, uncorrelated and unit standard deviation. The constant C is chosen, so that $C = \sigma$, where σ is the standard deviation of measured temperatures.

The first attempt in order to resolve the inverse problem can be the identification of measured temperatures $\mathbf{Y}$ with the calculated temperatures $\mathbf{T}$ expressed by Eq. (4), so that the unknown vector $\mathbf{q}$ can be obtained from

$$\mathbf{q} = [\mathbf{X}]^{-1} b \quad \text{where } \mathbf{b} = (\mathbf{Y} - \mathbf{T}_0) \tag{5}$$

We note that diagonal coefficients of $[\mathbf{X}]$ are equal to $\Delta\phi_0$. This sensitivity coefficient represents the response (at $x = 1$) to a unitary pulse (with a wideness of one time step), just when the pulse has finished. If the time step is sufficiently small, this response can be several orders of magnitude lower than others sensitivity values. This justifies (from a physical point of view) that $[\mathbf{X}]$ is an ill-conditioned matrix. On the other hand, as $\mathbf{Y}$ is affected by measurements errors, the estimation of $\mathbf{q}$ by Eq. (5) will be unstable. In this study we consider three possible methods in order to get a stable algorithm.

3.1. Beck's algorithm

As FSM is a sequential procedure, it is assumed that components: $\hat{q}_1, \hat{q}_1, \ldots, \hat{q}_{m-1}$, have been previously estimated (they are noted with "$\frown$"), and the objective is the estimation of the component q_m, corresponding to the m-time step (located in the time interval between t_{m-1} and t_m). The particular stabilisation technique of this method is based on the specification of the functional form corresponding to an unknown input $\mathbf{q}$. Since this method is sequential, the specification includes only r future steps from the last estimated component (component $m-1$). Then, the future components $q_m, q_{m+1}, \ldots, q_{m+r-1}$, can be written in terms of q_m, and only this component is estimated in each step. The temporal assumption can be made through several forms: constant, linear, parabolic, etc. In this paper the simplest form is used, and hence the r future components are assumed temporarily constant. Details of this algorithm can be seen in Ref. [6]. The estimated component, noted as $\hat{q}_m$ can be expressed as

$$\hat{q}_m = \frac{\sum_{j=0}^{r-1} (Y_{m+j} - \sum_{n=0}^{m-1} \hat{q}_n \Delta\phi_{m-n+j} - T_0) C_{0j}}{\sum_{j=0}^{r-1} C_{0j}^2} \tag{6}$$

where $C_{0j} = \sum_{l=0}^{j} \Delta\phi_{j-l}$ and $q_0 = 0$.

3.2. SVD algorithm

In order to avoid the difficulties derived from the matrix inversion in Eq. (5), the singular value decomposition [19] of $[\mathbf{X}]$ is considered, so that this sensitivity matrix can be expressed as

$$[\mathbf{X}] = [\mathbf{U}][\mathbf{S}][\mathbf{V}]^{\mathrm{T}} \tag{7}$$

where $[\mathbf{U}]$ and $[\mathbf{V}]$ are orthogonal matrices which columns vectors are the eigenvectors of $[\mathbf{X}] \cdot [\mathbf{X}]^{\mathrm{T}}$ and $[\mathbf{X}]^{\mathrm{T}} \cdot [\mathbf{X}]$, respectively. These vectors will be noted as $\mathbf{u}_i$ and $\mathbf{v}_i$, and are called left and right singular vectors of $[\mathbf{X}]$. The diagonal matrix $[\mathbf{S}] = \mathrm{diag}[\lambda_1, \lambda_2, \ldots, \lambda_M]$ contains the square root of the eigenvalues of $[\mathbf{X}] \cdot [\mathbf{X}]^{\mathrm{T}}$. These coefficients (noted as λ_i) are arranged in decreasing magnitude and are called the singular values of $[\mathbf{X}]$. The factorisation given by Eq. (7) can be expressed as an outer product expansion [26]:

$$[\mathbf{X}] = [\mathbf{U}][\mathbf{S}][\mathbf{V}]^{\mathrm{T}} = \sum_{i=1}^{M} \lambda_i \mathbf{u}_i \mathbf{v}_i^{\mathrm{T}} \tag{8}$$

In this expression, the matrix $[\mathbf{X}]$, of rank M and dimension $M \times M$, is decomposed as the sum of M matrices of rank 1 and dimension $M \times M$. This expansion is known as *Spectral Decomposition*. The condition number of this matrix is the ratio: $CN = \lambda_1/\lambda_M$, so that matrices with $CN \gg 1$ are ill-conditioned.

The factorisation SVD presents important properties, interpretations and applications. One of the most interesting applications in the ill-posed problems in order to get a reduced model, is based on the reduced rank approximations. If expansion (8) is truncated to the p-first singular values and the corresponding left and right singular vectors (truncated SVD), the new matrix and the corresponding factorisation (noted by the subscript $_{\mathrm{red}}$) will be expressed as

$$[\mathbf{X}_{\mathrm{red}}] = [\mathbf{U}_{\mathrm{red}}][\mathbf{S}_{\mathrm{red}}][\mathbf{V}_{\mathrm{red}}]^{\mathrm{T}} = \sum_{i=1}^{p} \lambda_i \mathbf{u}_i \mathbf{v}_i^{\mathrm{T}} \quad p < M \tag{9}$$

Golub [19] shows that $[\mathbf{X}_{\mathrm{red}}]$ is the closest matrix to $[\mathbf{X}]$ that has rank p. With an adequate effective rank p, the approximation of $[\mathbf{X}]$ by $[\mathbf{X}_{\mathrm{red}}]$ presents a notable advantage in order to solve a direct and an inverse problem. In the direct problem the $M - p$ smallest terms of the sum (8) have a negligible contribution, and in the inverse problem, the elimination of the same terms, reduces the condition number and the numerical instability.

On the other hand, this rank reduction has a physical interpretation based on the discussion of the data filtering in frequency-domain. If we consider the SVD of matrix $[\mathbf{X}]$, then Eq. (5) can be expressed by

$$\begin{aligned} \mathbf{q} &= [\mathbf{X}]^{-1}\mathbf{b} = [\mathbf{V}][\mathbf{S}]^{-1}[\mathbf{U}]^{\mathrm{T}}\mathbf{b} \\ &= \sum_{i=1}^{M} \frac{1}{\lambda_i} \mathbf{v}_i \mathbf{u}_i^{\mathrm{T}} \mathbf{b} = \sum_{i=1}^{M} c_i \mathbf{v}_i \end{aligned} \tag{10}$$

where $c_i = \frac{1}{\lambda_i}\beta_i$, $\beta_i = \mathbf{u}_i^{\mathrm{T}}\mathbf{b}$ and $\mathbf{b} = \mathbf{Y} - \mathbf{T}_0$.

In Eq. (10), $\mathbf{q}$ is expressed as a linear combination of the orthonormal vectors $\mathbf{v}_i$. The coefficient c_i is pondered by the factors $1/\lambda_i$ and the convolution between the components of columns vectors $\mathbf{u}_i$ and measured temperatures vector $\mathbf{b}$. In agreement with Shenefelt [24], vectors $\mathbf{u}_i$ act upon the measured temperature, $\mathbf{b}$, as a band-pass filter, so that the band is displaced toward high frequencies as the number of columns is increased. The band pass-filters corresponding to high frequencies of random noise, might be removed because in those frequency ranges, the inverse of the smallest singular values $1/\lambda_i$ are very large, and this provoke a great amplification of measurement errors. Hence, the SVD algorithm (corresponding to the whole domain procedure) can be expressed as

$$\hat{\mathbf{q}} = [\mathbf{X}_{\text{red}}]^{-1}\mathbf{b} = [\mathbf{V}_{\text{red}}][\mathbf{S}_{\text{red}}]^{-1}[\mathbf{U}_{\text{red}}]^{\text{T}}\mathbf{b} = \sum_{i=1}^{p} \frac{1}{\lambda_i}\mathbf{v}_i\mathbf{u}_i^{\text{T}}\mathbf{b} \quad p < M \tag{11}$$

With an adequate reduced rank we get a good ratio signal-to-noise. As it is expected, the optimum p-value is very dependent on the frequency components of the unknown input.

3.3. Sequential SVD algorithm

In similar form to FSM, the sequential algorithm SVD uses the r future temperatures (measured and calculated), nevertheless the stabilisation technique is not based on the specification of the unknown input. In order to obtain the sequential algorithm SVD, we consider the Eq. (4), extended to r future steps from the last estimated component (component $m-1$). In a partitioned form, the matrix equation can be written as

$$\begin{bmatrix}\mathbf{T}_{\text{past}}\\ \mathbf{T}_{\text{fut}}\end{bmatrix} = \begin{bmatrix}\mathbf{X}_{\text{past}} & 0\\ \mathbf{H} & \mathbf{X}_{\text{fut}}\end{bmatrix}\begin{bmatrix}\hat{\mathbf{q}}_{\text{past}}\\ \mathbf{q}_{\text{fut}}\end{bmatrix} + \mathbf{T}_0 \tag{12}$$

where the vectors are

$$\mathbf{T}_{\text{past}} = [T_1 \dots T_{m-1}]^{\text{T}}, \qquad \mathbf{T}_{\text{fut}} = [T_m \dots T_{m+r-1}]^{\text{T}}$$
$$\hat{\mathbf{q}}_{\text{past}} = [\hat{q}_1 \dots \hat{q}_{m-1}]^{\text{T}}, \qquad \mathbf{q}_{\text{fut}} = [q_m \dots q_{m+r-1}]^{\text{T}}$$

and the matrices are

$$[\mathbf{X}_{\text{past}}] = \begin{bmatrix}\Delta\phi_0 & 0 & \dots & 0\\ \Delta\phi_1 & \Delta\phi_0 & \dots & 0\\ \vdots & \vdots & \ddots & \vdots\\ \Delta\phi_{m-2} & \Delta\phi_{m-3} & \cdots & \Delta\phi_0\end{bmatrix}$$

$$[\mathbf{H}] = \begin{bmatrix}\Delta\phi_{m-1} & \Delta\phi_{m-2} & \dots & \Delta\phi_1\\ \Delta\phi_m & \Delta\phi_{m-1} & \dots & \Delta\phi_2\\ \vdots & \vdots & \ddots & \vdots\\ \Delta\phi_{m+r-2} & \Delta\phi_{m+r-3} & \dots & \Delta\phi_r\end{bmatrix}$$

$$[\mathbf{X}_{\text{fut}}] = \begin{bmatrix}\Delta\phi_0 & 0 & \dots & 0\\ \Delta\phi_1 & \Delta\phi_0 & \dots & 0\\ \vdots & \vdots & \ddots & \vdots\\ \Delta\phi_{r-1} & \Delta\phi_{r-2} & \dots & \Delta\phi_0\end{bmatrix}$$

Notice that future temperatures can be written as

$$\underset{r\times 1}{\mathbf{T}_{\text{fut}}} = \underset{r\times m-1}{[\mathbf{H}]}\ \underset{m-1\times 1}{\hat{\mathbf{q}}_{\text{past}}} + \underset{r\times r}{[\mathbf{X}_{\text{fut}}]}\ \underset{r\times 1}{\mathbf{q}_{\text{fut}}} + \underset{r\times 1}{\mathbf{T}_0} \tag{13}$$

where the previous history is stored in matrix $[\mathbf{H}]$ and vector $\hat{\mathbf{q}}_{\text{hist}}$. The vectors and matrix related with future temperatures are: $\mathbf{T}_{\text{fut}}$, $\mathbf{q}_{\text{fut}}$ and $[\mathbf{X}_{\text{fut}}]$. Considering the identification between $\mathbf{T}_{\text{fut}}$ and $\mathbf{Y}_{\text{fut}}$, we obtain

$$\mathbf{q}_{\text{fut}} = [\mathbf{X}_{\text{fut}}]^{-1}\mathbf{b} \tag{14}$$

now the vector $\mathbf{b}$ is given by

$$\mathbf{b} = \mathbf{Y}_{\text{fut}} - [\mathbf{H}]\hat{\mathbf{q}}_{\text{past}} - \mathbf{T}_0 \tag{15}$$

Taking into account Eq. (13), the expression: $[\mathbf{H}]\hat{\mathbf{q}}_{\text{past}} + \mathbf{T}_0$ can be interpreted as the calculated temperature over $t_{m-1} \leqslant t \leqslant t_{m+r-1}$, considering that in this time interval the input is held at zero. This concept is noted as $[\mathbf{H}]\hat{\mathbf{q}}_{\text{past}} + \mathbf{T}_0 = \mathbf{T}|_{\mathbf{q}_{\text{fut}}=0}$, so that the data vector is $\mathbf{b} = \mathbf{Y}_{\text{fut}} - \mathbf{T}|_{\mathbf{q}_{\text{fut}}=0}$.

Following, we consider the SVD of the small sensitivity matrix $[\mathbf{X}_{\text{fut}}]$

$$\underset{r\times r}{[\mathbf{X}_{\text{fut}}]} = [\mathbf{U}][\mathbf{S}][\mathbf{V}]^{\text{T}} = \sum_{i=1}^{r} \lambda_i \mathbf{u}_i \mathbf{v}_i^{\text{T}} \tag{16}$$

In order to get a stable algorithm, we consider the closest matrix to $[\mathbf{X}_{\text{fut}}]$ that has rank p. This matrix, called $[\mathbf{X}_{\text{red}}]$, will be given by

$$\underset{r\times r}{[\mathbf{X}_{\text{red}}]} = [\mathbf{U}_{\text{red}}][\mathbf{S}_{\text{red}}][\mathbf{V}_{\text{red}}]^{\text{T}} = \sum_{i=1}^{p} \lambda_i \mathbf{u}_i \mathbf{v}_i^{\text{T}} \quad p < r \tag{17}$$

and with an adequate p-value, we obtain a stable algorithm

$$\hat{\mathbf{q}}_{\text{fut}} = [\mathbf{X}_{\text{red}}]^{-1}\mathbf{b} = [\mathbf{V}_{\text{red}}][\mathbf{S}_{\text{red}}]^{-1}[\mathbf{U}_{\text{red}}]^{\text{T}}\mathbf{b} = \sum_{i=1}^{p} \frac{1}{\lambda_i}\mathbf{v}_i\mathbf{u}_i^{\text{T}}\mathbf{b} \quad p < r \tag{18}$$

According to Eq. (18), the sequential SVD algorithm presents two tunable hyperparameters r and p. For a given p-value, we can carry out numerical experiments in order to find the corresponding optimum r-value. This optimum value is obtained from the minimization of the total error S, given by Eq. (23). The numerical experiments given in Section 4, show that the most suitable reduced rank is $p = 1$. Greater ranks ($p > 1$) require larger optimal r-values. This fact represents a disadvantage in an on-line process, because the time period $r_{\text{opt}} \cdot \Delta t$ (named as "look ahead" [28]) can be excessively long. The expression of the data vector $\mathbf{b}$ is crucial to justify the advantage of sequential SVD algorithm under the assumption $p = 1$. In the whole domain procedure, the components of $\mathbf{b}$ are the measured temperatures (with respect to the initial temperature). Normally, in these data set the signal amplitude is much higher than the noise one. On the other hand, the data vector corresponding to the sequential procedure is $\mathbf{b} = \mathbf{Y}_{\text{fut}} - \mathbf{T}|_{\mathbf{q}_{\text{fut}}=0}$. Comparing the data vector used in each procedure, we can state that:

- Due to $r \ll M$, the dimension of $\mathbf{b}$ is much smaller in the sequential procedure.
- Due to thermal inertia of heat conduction, the components of $\mathbf{Y}_{\text{fut}}$ and $\mathbf{T}|_{\mathbf{q}_{\text{fut}}=0}$ give similar values.
- $\mathbf{Y}_{\text{fut}}$ and $\mathbf{T}|_{\mathbf{q}_{\text{fut}}=0}$ are affected by errors. The first is affected directly by measurement errors. The second depends on $\hat{\mathbf{q}}_{\text{past}}$, and it is an estimated vector affected by two types of errors: stochastic (consequence of the measurement errors) and deterministic (consequence of the approximation in order to get a stable estimation).
- When $\mathbf{Y}_{\text{fut}}$ and $\mathbf{T}|_{\mathbf{q}_{\text{fut}}=0}$ are subtracted to give $\mathbf{b}$, the components of $\mathbf{b}$ are small numbers, and as consequence of the errors, they presents fluctuations. In this case, the signal amplitude is of the same magnitude order than the noise one.

According to the data filtering interpretation of Shenefelt [24], the fact that sequential SVD algorithm gives satisfactory results (in all cases considered in this study) when $p = 1$, means that the most relevant information is contained in the lowest frequency components of the Fourier series of $\mathbf{b}$. Consequently, under this assumption ($p = 1$), the unique tunable hyperparameter is the number of future temperatures r. The regularization effect of r, will be considered in the next section. Assuming that SVD can be calculated numerically with an efficient code [27], it is possible to obtain a very simple algorithm. When $p = 1$, Eq. (18) is reduced to

$$\hat{\mathbf{q}}_{\text{fut}} = \mathbf{v}_1 \frac{1}{\lambda_1} \mathbf{u}_1^{\mathrm{T}} \mathbf{b} \tag{19}$$

where $\mathbf{v}_1 = [v_{11}, \ldots, v_{r1}]^{\mathrm{T}}$, $\mathbf{u}_1^{\mathrm{T}} = [u_{11}, \ldots, u_{r1}]$, $\mathbf{b} = [b_1, \ldots, b_r]^{\mathrm{T}}$, and $\hat{\mathbf{q}}_{\text{fut}} = [\hat{q}_m, \ldots, \hat{q}_{m+r-1}]^{\mathrm{T}}$. Taking into account the sequential characteristic of this method, only the first component $\hat{q}_m$ is retained. This calculus process is repeated for the next time step. Finally, the sequential SVD algorithm can be expressed as

$$\hat{q}_m = \frac{1}{\lambda_1} v_{11} \sum_{i=1}^{r} b_i u_{i1} \tag{20}$$

4. Results and discussions

In an IHCP there are two sources of error in the estimation. The first source is the unavoidable bias deviation (or deterministic error). The second source of error is the variance due to the amplification of measurement errors (stochastic error). The global effect of deterministic and stochastic errors is considered in the mean squared error or total error. The estimates used in this study for the bias (D), the variance (σ_q) and the total error (S) are defined by Eqs. (21)–(23), respectively.

$$D = \left[\frac{1}{N-1} \sum_{i=1}^{N} \left(\hat{q}_i|_{\sigma=0} - q_i \right)^2 \right]^{1/2} \tag{21}$$

Table 1
Comparison of error estimations for different inverse algorithms and several cases

Algorithm	D	σ_q	S
Case 1: $\sigma = 0.001$, $r = 7$, $\Delta t = 0.03$			
FSM ○	0.0109	0.0104	0.0157
Seq.-SVD •	0.0143	0.0134	0.0197
SVD □	0.0066	0.0050	0.0083
Case 2: $\sigma = 0.01$, $r = 12$, $\Delta t = 0.03$			
FSM ○	0.0344	0.0242	0.0390
Seq.-SVD •	0.0373	0.0299	0.0428
SVD □	0.0163	0.0091	0.0188
Case 3: $\Delta t = 0.1$, $r = 2$, $\sigma = 0.001$			
FSM ○	0.0823	0.0282	0.0939
Seq.-SVD •	0.0654	0.0343	0.0794
SVD □	0.0081	0.0416	0.0424
Case 4: $\Delta t = 0.03$, $r = 5$, $\sigma = 0.001$			
FSM ○	0.1171	0.0359	0.1191
Seq.-SVD •	0.1148	0.0480	0.1197
SVD □	0.0996	0.0345	0.1054
Case 5: $\sigma = 0.001$, $r = 9$, $\Delta t = 0.025$			
FSM ○	0.0099	0.0081	0.0116
Seq.-SVD •	0.0131	0.0102	0.0153
SVD —□—	0.1912	0.0392	0.1952

$$\sigma_q = \left[\frac{1}{N-1} \sum_{i=1}^{N} \left(\hat{q}_i - \hat{q}_i|_{\sigma=0} \right)^2 \right]^{1/2} \tag{22}$$

$$S = \left[\frac{1}{N-1} \sum_{i=1}^{N} \left(\hat{q}_i - q_i \right)^2 \right]^{1/2} \tag{23}$$

where N is the total number of estimated values. The best estimation is obtained from the minimization of total error S, which gives the necessary balance between the two error sources [6]. This criterion is very useful in a comparative study (as the actual). Nevertheless, in a practical case, the residual principle [8] provides a more realistic criterion. It must be pointed out that sequential algorithms (FSM and sequential SVD) use r measurements before heating starts ($t < 0$). In accordance with Beck [6], this is performed in order to minimise the effect of the anomalous calculation during the first few steps. In the whole domain SVD, the previous measurements are not required, nevertheless they have been included in order to do a comparison point-by-point.

A total of five cases are summarised in Table 1. The results correspond to the best estimation obtained by FSM, the standard whole-domain SVD and sequential SVD (using $p = 1$). Before the comparative analysis, we present a discussion about the tunable hyperparameters p and r of the sequential SVD algorithm.

Consider the case 1 of Table 1. This case corresponds to a triangular test where, $\sigma = 0.001$, and $\Delta t = 0.03$. If $p = 1$ the condition number (CN) of the matrix X_{red} is $CN = 1$, and the best estimation is obtained when $r_{\text{opt}} = 7$. The error estimations are (see Table 1): $D = 0.0143$, $\sigma_q = 0.0134$

and $S = 0.0197$. If $r < r_{opt}$, for example, $r = 3$, then the error estimations are: $D = 0.0008$, $\sigma_q = 0.4629$ and $S = 0.46304$. In this extreme case, the estimation is very deficient. The dominant error is due to the great amplification of the measurement errors. If $r > r_{opt}$, for example, $r = 20$, then the error estimations are: $D = 0.0764$, $\sigma_q = 0.0009$ and $S = 0.0763$. In this extreme case, the dominant error is the bias. Note that CN of X_{red} is the same in all cases ($CN = 1$). X_{red} is a matrix of $r \times r$, but the rank is $p = 1$. Numerical results show that as r-value is augmented, the damping effect is more significant. This is consistent with the data filtering interpretation of Shenefelt [24]. According to Shenefelt, $\mathbf{u}_1^T$ acts upon vector $\mathbf{b}$ as a band-pass filter. The power spectral density corresponding to the components of vector $\mathbf{u}_1^T$, reveals that the wideband of the band-pass filter depends on r-value. Obviously, the most suitable wideband in order to get the signal reconstruction, corresponds to $r = r_{opt}$, but if $r < r_{opt}$ the wideband is increased, and as it is expected, the high frequencies of random noise are not filtered. If $r > r_{opt}$, the opposite occurs, so that the amplification factor of measurement errors can be negligible, but the bias is increased. This fact justifies the regularization effect of r-value on the previous examples. Similar numerical behaviour is observed in other test cases.

Following we treat the effect of the reduced rank p. With this purpose we consider the same prior case (case 1 of Table 1) but with a reduced rank $p = 2$. If $r = 7$ (this value corresponds to r_{opt} when $p = 1$), the condition number of matrix X_{red} is $CN = 5.78$. As it is well known, the CN quantifies the sensitivity of a linear system [19]. The error estimations of this case are: $D = 0.0033$, $\sigma_q = 0.0939$ and $S = 0.0939$. Comparing this estimation with the corresponding to case 1 of Table 1, now, CN of X_{red} has been increased (when $p = 1$ $CN = 1$), consequently, the system is more sensible to the measurements errors. On the other hand, now $p = 2$ and $CN = \lambda_1/\lambda_2$. This implies that CN is sensible to the number r of future temperature used. If $p = 2$, Eq. (18) includes two vectors $\mathbf{u}_1^T$ and $\mathbf{u}_2^T$, therefore now we are considering two band-pass filters. The second filter ($\mathbf{u}_2^T$) permits the amplification of larger frequencies than the first filter, consequently the best estimation for $p = 2$ requires grater r-value (or smaller wideband) in order to reduce σ_q and CN. The optimum r-value for $p = 2$ is $r = 14$, and the corresponding error estimations and CN are: $D = 0.0121$, $\sigma_q = 0.0082$, $S = 0.0140$, and $CN = 4.15$. If we compare these results to the corresponding to case 1 of Table 1, we conclude that the estimation is similar (or slightly more accurate), but the look ahead time period now is double, so that the insignificant differences in the estimations error, do not justify the use of the sequential SVD algorithm with $p > 1$. The numerical behaviour with respect to p-value is similar in other test.

Following we consider the comparative study. Cases 1 and 2, show the effect of noise level in measurement errors through a triangular test. Two levels of noise measurements $\sigma = 0.001$ (case 1) and $\sigma = 0.01$ (case 2) are considered.

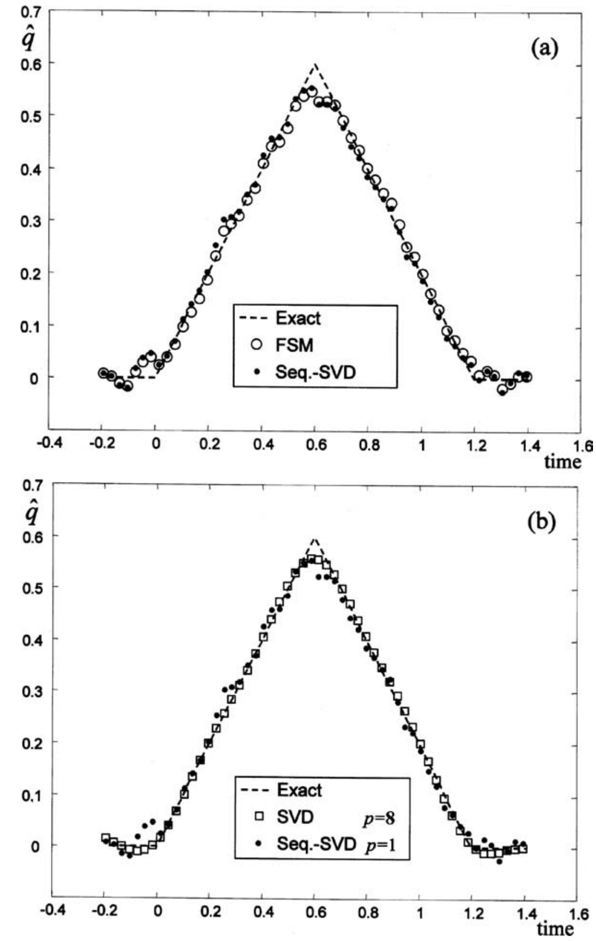

Fig. 2. Case 1: $\sigma = 0.001$, $r = 7$, $\Delta t = 0.03$: (a) Comparison between FSM and Seq.-SVD; (b) Comparison between SVD and Seq.-SVD.

Taking as reference the maximum increase of dimensionless temperature (0.3581) at location sensor ($x = 1$), and considering (around the exact temperatures) an error range between $\pm 2.576\sigma$ (or 99% confidence interval), these noise levels correspond to error percentages of 0.72 and 7.2%, respectively. In both cases, the dimensionless time step has been $\Delta t = 0.03$. Case 1, corresponds to Fig. 2(a) and (b). Fig. 2(a) compares the results corresponding to the best estimation obtained by FSM and sequential SVD (noted as Seq.-SVD). In both methods the number of future temperatures has been $r = 7$. We note that in all cases considered, the optimum r-value is coincident in both sequential methods. Fig. 2(b) compares the results corresponding to the best estimation obtained by Seq.-SVD, and whole domain SVD (noted as SVD), respectively. The initial rank corresponding to sensitivity matrix in the whole domain procedure is 64, and the optimum reduced rank has been $p = 8$. Comparing the graphical representations and the error estimates (Table 1, case 1), the results obtained by the two sequential procedures are very similar. The components of Fourier series corresponding to the triangular input are very dominant in the range of low frequencies. This justifies why the whole domain SVD algorithm provides slightly more ac-

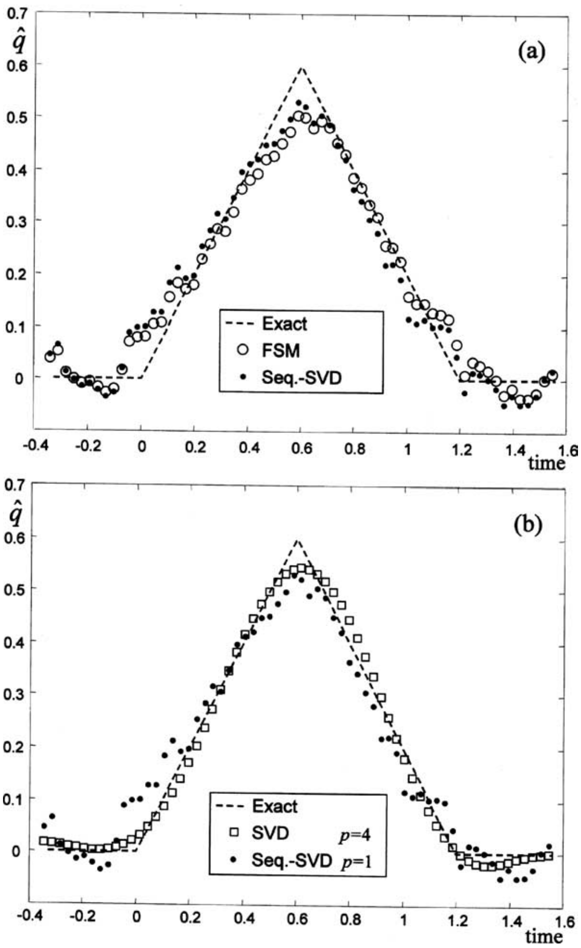

Fig. 3. Case 2: $\sigma = 0.01$, $r = 12$, $\Delta t = 0.03$: (a) Comparison between FSM and Seq.-SVD; (b) Comparison between SVD and Seq.-SVD.

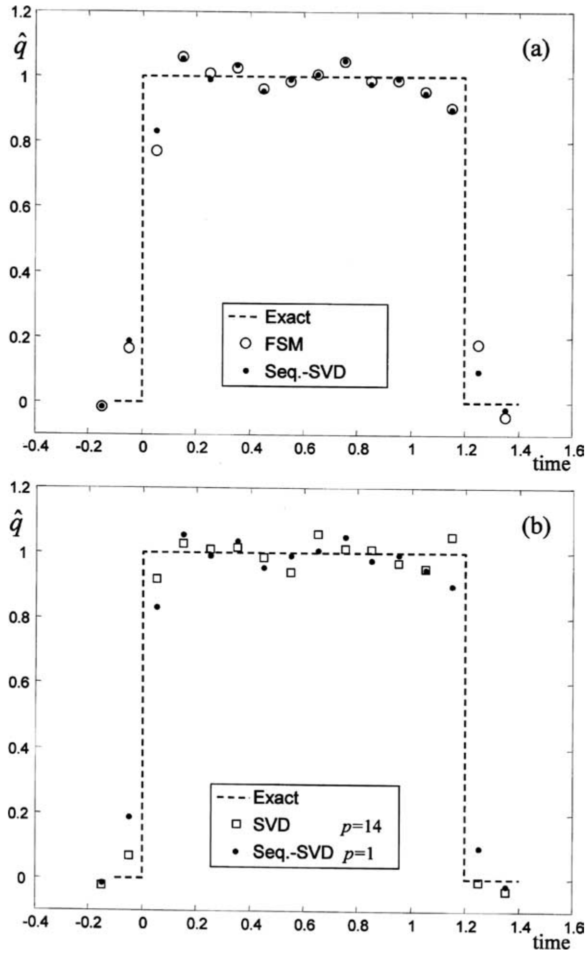

Fig. 4. Case 3: $\Delta t = 0.1$, $r = 2$, $\sigma = 0.001$: (a) Comparison between FSM and Seq.-SVD; (b) Comparison between SVD and Seq.-SVD.

curate results. Similar conclusions are obtained in case 2. As expected, a greater noise level requires a greater r-value ($r = 12$ in the sequential methods), and a smaller rank (or a more "severe" filter) ($p = 4$ in whole domain SVD).

In cases 3 and 4, the effect of the dimensionless time step size through a rectangular test has been considered. In both cases, the noise level has been $\sigma = 0.001$. Case 3 refers to a relatively large dimensionless time step $\Delta t = 0.1$. Because of its size, only $N = 16$ measurements are included. As expected, large time step requires small number of future temperatures. The best estimation is obtained with $r = 2$. Nevertheless when $r = 1$, the estimation is unstable. In this test, the dissimilarities among the three methods are less significant than in the triangular test. A similar conclusion is obtained when the size of time step is decreased ($\Delta t = 0.03$). As expected, shorter time step requires larger r-value in order to assure the stability. Considering the whole domain SVD algorithm, the comparison between the results of the triangular test (Fig. 2(b)) and the rectangular test (Fig. 5(b)) (both cases with the same time step and noise level), shows that the rectangular test requires a larger p-value. This justifies the greater amplification observed in the measurement errors.

Finally, case 5 shows a weakness of the whole domain SVD. The reconstruction of this test requires the little contribution of some components in the range of high frequencies. Consequently the p-value ($p = 23$) cannot be as smaller as in the triangular test ($p = 8$). If the reduction of rank is not drastic, the inverse of the smaller singular values $1/\lambda_i$ cause a notable amplification of measurements errors in the inverse problem. These circumstances can be seen in this case (Table 1, case 5). Fig. 6(a), shows the estimations by the two sequential methods. They are excellent and very similar. On the other hand, Fig. 6(b) shows that the estimation by the whole domain SVD is very inferior to the corresponding by sequential SVD.

5. Conclusions

In this paper we have presented a study about the application of truncated SVD in a sequential form. The regularization effect of the hyperparameters p and r is consistent with the data filtering interpretation by truncated SVD. The principal regularization effect is carried out by the reduced rank p. This implies the elimination of the band-pass filters corre-

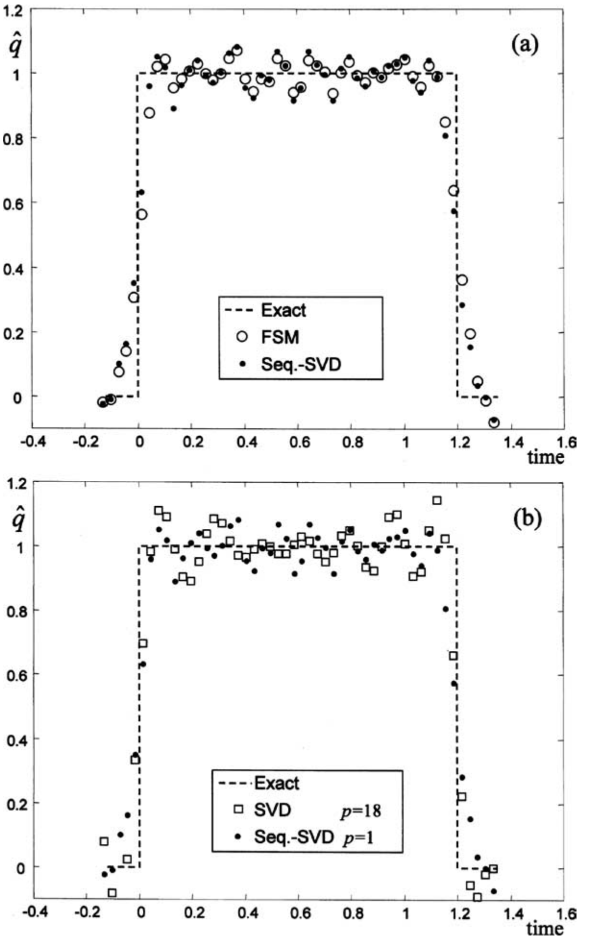

Fig. 5. Case 4: $\Delta t = 0.03$, $r = 5$, $\sigma = 0.001$: (a) Comparison between FSM and Seq.-SVD; (b) Comparison between SVD and Seq.-SVD.

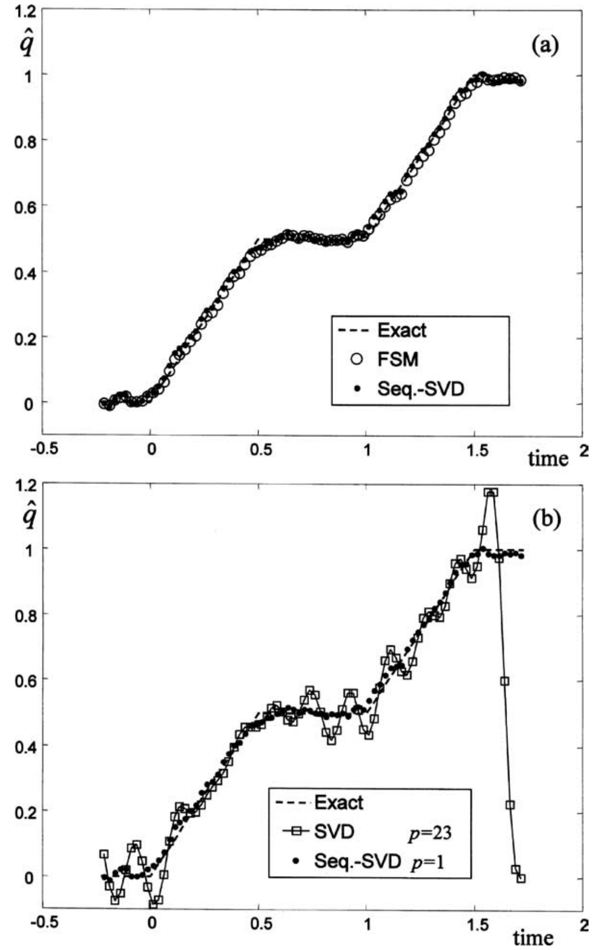

Fig. 6. Case 5: $\sigma = 0.001$, $r = 9$, $\Delta t = 0.025$: (a) Comparison between FSM and Seq.-SVD; (b) Comparison between SVD and Seq.-SVD.

sponding to high frequencies of random noise. Additionally, the sequential algorithm presented in this study, permits the control of the wideband with the number of future temperature r. This study reveals that the most suitable reduced rank is $p = 1$. Greater ranks ($p > 1$) provide similar accuracy but require larger optimal r-values (or larger look ahead time period). In other words, the most simple model with a unique band-pass filter ($p = 1$) and a great wideband (or a reduced r-value) is quasi-equivalent to a more complex model with several band-pass filters ($p > 1$) and a smaller wide-band (or largest r-value).

Five cases have been used in order to compare the sequential SVD algorithm, using $p = 1$, to a sequential algorithm based in the FS method, and to the standard whole-domain SVD method. Considering the comparison carried out with the FS method, the following conclusions can be drawn:

- In both algorithms, the unique tunable hyperparameter is the number of future temperatures r.
- In all the cases considered, the optimum r-value is the same for the two algorithms.
- Although the stabilisation techniques are different, both sequential algorithms give very similar results.

If we consider the comparison between sequential estimation using SVD (and $p = 1$) and the whole domain estimation using SVD:

- The search of the optimum rank value (p) is not required in the sequential SVD.
- As the sequential SVD uses $p = 1$ in all cases, the simplification of the model is the maximum that can be achieved. This fact allows to obtain a very simple algorithm.
- The whole domain algorithm provides the best estimations when the components of Fourier series of the unknown input are very dominant in the range of low frequencies. In other circumstances, the estimation can be deficient. In contrast, the sequential SVD algorithm assures a reasonable estimation in all cases.

Acknowledgements

This work is supported in part by a grant from the Andalusian Government through P.A.I. (Group TEP-157). The authors would like to thank Prof. Dr. L. Cohen Mesonero and Prof. F.J. González Gallero for their help to improve the English text. We also thank Dr. I. Rodríguez Maestre for useful discussions. Finally, the authors are very grateful for the helpful comments and suggestions offered by reviewers.

References

[1] O.V. Nagornov, Yu.V. Konovalov, V.S. Zagorodonov, L.G. Thompsom, Reconstruction of the Surface Temperature of Artic Glaciers from the data of temperature measurement, J. Engrg. Phys. Thermophys. 74 (2001) 253–265.

[2] M. Janicki, M. Zubert, A. Napieralski, Application of inverse problem algorithms for integrated circuit temperature estimation, Microelectronic J. 30 (1999) 1099–1107.

[3] F. Rosa, A. Valverde, J.M. Aranda, J. Aranda, J. Rodríguez, CESA-1 Project capabilities for high temperature material testing: Application to the Hermes wing leading edge tests, Solar Energy 46 (1991) 175–182.

[4] T.-G. Kim, Z.-H. Lee, Time-varying heat transfer coefficients between tube-shaped casting and metal mold, Internat. J. Heat Mass Transfer 40 (1997) 3513–3525.

[5] J. Lin, Inverse estimation of the tool-work interface temperature in end milling, Internat. J. Mach. Manufact. 35 (1995) 751–760.

[6] J.V. Beck, B. Blackwell, C.R. St. Clair, Inverse Heat Conduction: Ill Posed Problems, Wiley–Interscience, New York, 1985.

[7] A.N. Tikhonov, V.Y. Arsenin, Solution of Ill-Posed Problems, Winston & Sons, Washington, DC, 1977.

[8] O.M. Alifanov, Inverse Heat Transfer Problems, Springer, New York, 1994.

[9] D.A. Murio, The Mollification Method and the Numerical Solution of Ill-Posed Problems, Wiley–Interscience, New York, 1993.

[10] J.V. Beck, D.C. Murio, Combined function specification-regularization procedure for solution of inverse heat conduction problem, AIAA J. 24 (1986) 180–185.

[11] D.C. Murio, J.R. Paloschi, Combined mollification-future temperatures procedure for solution of inverse heat conduction problem, J. Comput. Appl. Math. 23 (1988) 235–244.

[12] N. Zabaras, J.C. Liu, An analysis of two-dimensional linear inverse heat transfer problems using an integral method, Numer. Heat Transfer 13 (1990) 527–533.

[13] G. Blanc, J.V. Beck, M. Raynaud, Solution of the inverse heat conduction problem with a time-variable numbers of future temperatures, Numer. Heat Transfer B 32 (1997) 437–451.

[14] J.V. Beck, B. Blackwell, A. Haji-Sheikh, Comparison of some inverse heat conduction methods using experimental data, Internat. J. Heat Mass Transfer 39 (1996) 3649–3657.

[15] R.E. Kalman, A new approach to linear filtering and prediction problems, ASME J. Basic Engrg. Ser. B 82 (1960) 35–45.

[16] Yu.M. Matsevityi, V.A. Maliarenko, A.V. Multanovskii, Identification of time-variable coefficients of heat transfer by solving a nonlinear inverse problem of heat conduction, J. Engrg. Phys. 35 (1979) 1094–1098.

[17] N. Daouas, M.-S. Radhouani, Versión étendue du filtre de Kalman discret appliquée à un problème inverse de conduction de chaleur non linéaire, Internat. J. Therm. Sci. 39 (2000) 191–212.

[18] S.S. Shyam, A neural network approach for non-iterative calculation of heat transfer coefficient in fluid-particle systems, Chem. Engrg. Processing 40 (2001) 363–369.

[19] G.H. Golub, C.F. Van Loan, Matrix Computations, John Hopkins University Press, Baltimore, MD, 1983.

[20] T.J. Martin, G.S. Dulikravich, Inverse determination of boundary conditions and sources in steady heat conduction with heat generation, ASME J. Heat Transfer 118 (1996) 546–554.

[21] T.J. Martin, G.S. Dulikravich, Inverse determination of steady heat convection coefficient distributions, ASME J. Heat Transfer 120 (1998) 328–334.

[22] S.-Y. Shen, A numerical study of inverse heat conduction problems, Comput. Math. Appl. 38 (1999) 173–188.

[23] W.B. Muniz, F.M. Ramos, F. De Campos, Entropy and Tikhonov-based regularization techniques applied to the backwards heat equation, Comput. Math. Appl. 40 (2000) 1071–1084.

[24] J.R. Shenefelt, R. Luck, R.P. Taylor, J.T. Berry, Solution to inverse heat conduction problems employing singular value decomposition and model-reduction, Internat. J. Heat Mass Transfer 45 (2002) 67–74.

[25] H.S. Carslaw, J.C. Jaeger, Conduction of Heat in Solids, Oxford University Press, London, 1959.

[26] D. Kalman, A singularly Valuable Decomposition: The SVD of a Matrix, The American University, Washington, DC, 2002.

[27] W.H. Press, S.A. Teukolsky, W.T. Vetterling, B.P. Flannery, Numerical Recipes in Fortran, Cambridge University Press, Cambridge, 1992.

[28] K.A. Woodbory, S.K. Thakur, Redundant data, future times and sensor location in the IHCP: A case study, Inverse Problems Engrg. Mech. 2 (1996) 319–333.